The Journal of Immunology

Contrasting Roles for Domain 4 of VCAM-1 in the Regulation of Cell Adhesion and Soluble VCAM-1 Binding to Integrin $\alpha_4\beta_1$

Darren G. Woodside, Ronda M. Kram, Jason S. Mitchell, Tracie Belsom, Matthew J. Billard, Bradley W. McIntyre and Peter Vanderslice

J Immunol 2006; 176:5041-5049; ;
doi: 10.4049/jimmunol.176.8.5041
http://www.jimmunol.org/content/176/8/5041

The Journal of Immunology is published twice each month by
The American Association of Immunologists, Inc.,
1451 Rockville Pike, Suite 650, Rockville, MD 20852

Print ISSN: 0022-1767 Online ISSN: 1550-6606.

Contrasting Roles for Domain 4 of VCAM-1 in the Regulation of Cell Adhesion and Soluble VCAM-1 Binding to Integrin $\alpha_4\beta_1$[1]

Darren G. Woodside,[2]* Ronda M. Kram,* Jason S. Mitchell,† Tracie Belsom,* Matthew J. Billard,† Bradley W. McIntyre,† and Peter Vanderslice*

Cell adhesion mediated by the interaction between integrin $\alpha_4\beta_1$ and VCAM-1 is important in normal physiologic processes and in inflammatory and autoimmune disease. Numerous studies have mapped the $\alpha_4\beta_1$ binding sites in VCAM-1 that mediate cell adhesion; however, little is known about the regions in VCAM-1 important for regulating soluble binding. In the present study, we demonstrate that 6D VCAM-1 (an alternatively spliced isoform of VCAM-1 lacking Ig-like domain 4) binds $\alpha_4\beta_1$ with a higher relative affinity than does the full-length form of VCAM-1 containing 7 Ig-like extracellular domains (7D VCAM-1). In indirect binding assays, the EC_{50} of soluble 6D VCAM-1 binding to $\alpha_4\beta_1$ on Jurkat cells (in 1 mM $MnCl_2$) was 2×10^{-9} M, compared with 7D VCAM-1 at 11×10^{-9} M. When used in solution to inhibit $\alpha_4\beta_1$ mediated cell adhesion, the IC_{50} of 6D VCAM-1 was 13×10^{-9} M, compared with 7D VCAM-1 measured at 150×10^{-9} M. Removal of Ig-like domains 4, 5, or 6, or simply substituting Asp^{328} in domain 4 of 7D VCAM-1 with alanine, caused increased binding of soluble 7D VCAM-1 to $\alpha_4\beta_1$. In contrast, cells adhered more avidly to 7D VCAM-1 under shear force, as it induced cell spreading at lower concentrations than did 6D VCAM-1. Finally, soluble 6D VCAM-1 acts as an agonist through $\alpha_4\beta_1$ by augmenting cell migration and inducing cell aggregation. These results indicate that the domain 4 of VCAM-1 plays a contrasting role when VCAM-1 is presented in solution or as a cell surface-expressed adhesive substrate. *The Journal of Immunology,* **2006, 176: 5041–5049.**

The type I transmembrane glycoprotein VCAM-1 is a member of the Ig gene superfamily (1) and is involved in a number of different physiologic and pathological processes. It can be constitutively expressed or up-regulated on a variety of cell types including endothelial cells (1), fibroblasts from a variety of tissues (2–4), follicular dendritic cells (5), bone marrow stromal cells (6), and thymic epithelium (7). VCAM-1 plays a role in leukocyte transendothelial migration (reviewed in Refs. 8 and 9), leukocyte retention in tissues (10), and cellular activation (11, 12) by interaction with its primary cell surface ligand, the integrin cell adhesion molecule $\alpha_4\beta_1$ (13).

In humans, VCAM-1 is comprised of two isoforms (14). The full-length form of VCAM-1 contains 7 Ig-like extracellular domains (7D VCAM-1)[3] and is thought to be the predominant form expressed on the cell surface (14). An isoform of VCAM-1, 6D VCAM-1 (1), is a result of alternative splicing and lacks domain 4 (14). VCAM-1 can be released from the cell surface due to the activity of neutrophil-derived serine proteases such as neutrophil elastase and cathepsin G (15) or metalloproteases such as TNF-α converting enzyme (16). As such, increased concentrations of circulating VCAM-1 have been reported in patients with rheumatoid arthritis (17), multiple sclerosis (18), systemic lupus erythematosis (17), and sickle cell anemia (19). VCAM-1 has been found bound to integrin $\alpha_4\beta_1$ on synovial fluid T cells (20) and in solution has been reported to be chemotactic for T cells (21) and monocytes (22) and angiogenic for endothelial cells (23). By binding to integrin $\alpha_4\beta_1$, it can also enhance directed cell migration of lymphocytes on the integrin $\alpha_L\beta_2$ substrate ICAM-1 (24). It is currently unknown which isoform of VCAM-1 predominates in the circulation in the above disease states.

Although integrin $\alpha_4\beta_1$ can bind to domain 1 or domain 4 of VCAM-1 (25–27) to promote cell adhesion, binding is primarily mediated by residues within the NH_2-terminal domains in the intact, full-length 7D VCAM-1 (28, 29). An $\alpha_4\beta_1$ binding "footprint" has been characterized within VCAM-1 domains 1 and 2. This is composed of a primary binding site in domain 1 centered around a solvent-exposed loop created by anti-parallel β-strands (the C-D loop, which contains an essential Asp^{40} residue) and a secondary "synergy" site (the C′-E loop-E strand) in domain 2 (30). Although there has been much work focused on the key residues in VCAM-1 required for mediating $\alpha_4\beta_1$ integrin-dependent cell adhesion, very little work has focused on the molecular requirements for soluble VCAM-1 binding to $\alpha_4\beta_1$.

Cells bearing integrin $\alpha_4\beta_1$ adhere to the NH_2-terminal domains 1 and 2 of VCAM-1 (2D VCAM-1), independent of the intact molecule (30). However, as a soluble ligand, 2D VCAM-1 binds $\alpha_4\beta_1$ with a lower apparent affinity relative to full-length 7D VCAM-1 (31). This could be due to a second potential $\alpha_4\beta_1$ binding site within domain 4 of 7D VCAM-1 (25–27). To address this,

*Encysive Pharmaceuticals Incorporated, Houston, TX 77030; and †University of Texas M. D. Anderson Cancer Center, Houston, TX 77030

Received for publication February 3, 2005. Accepted for publication January 24, 2006.

The costs of publication of this article were defrayed in part by the payment of page charges. This article must therefore be hereby marked *advertisement* in accordance with 18 U.S.C. Section 1734 solely to indicate this fact.

[1] This work was supported in part by National Aeronautics and Space Administration Grant NAG2-1505 (to B.W.M.), the American Heart Association, Texas Affiliate (to B.W.M.), Predoctoral Cancer Immunobiology Training Program Grant CA09598 (to J.S.M. and M.J.B.), and an American Legion Auxiliary Fellowship (to J.S.M.).

[2] Address correspondence and reprint requests to Dr. Darren G. Woodside, Department of Molecular Pharmacology, Encysive Pharmaceuticals, 7000 Fannin, Houston, TX 77030. E-mail address: dwoodside@encysive.com

[3] Abbreviations used in this paper: 7D VCAM-1, full-length form of VCAM-1 containing 7 Ig-like extracellular domains; 6D VCAM-1, alternatively spliced isoform of VCAM-1 lacking Ig-like domain 4; 2D VCAM-1, NH_2-terminal domains 1 and 2 VCAM-1; RT, room temperature; CCD, charge-coupled device; MFI, mean fluorescence intensity.

0022-1767/06/$02.00

we generated a number of VCAM-1 constructs, including full-length 7D VCAM-1 and the alternatively spliced 6D VCAM-1, and tested their binding to integrin $\alpha_4\beta_1$. In the present study, we report the unexpected finding that 6D VCAM-1 bound $\alpha_4\beta_1$ with a higher relative affinity than did 7D VCAM-1 and that it was an efficient agonist of $\alpha_4\beta_1$ function. In contrast, as an adhesive substrate, 6D VCAM-1 was less efficient than 7D VCAM-1 in inducing cell spreading and in mediating cell adhesion under increasing shear force. Thus, as a soluble integrin $\alpha_4\beta_1$ agonist, 6D VCAM-1 may play a more important role than previously anticipated.

Materials and Methods

Cell lines

Jurkat clone E6.1 (American Type Culture Collection), the Jurkat cell line selected for loss of expression of the integrin α_4 subunit (Jurkat α_4^-) (32) (provided by D. Rose, University of California at San Diego, La Jolla, CA), Ramos (American Type Culture Collection), and HPB-ALL were grown in RPMI 1640 supplemented with 10% FBS, 100 U/ml penicillin, and 100 mg/ml streptomycin (complete medium) at 37°C, 5% CO_2, in a humidified atmosphere. Peripheral blood T cells were purified from the buffy coats (Gulf Coast Regional Blood Center) of healthy donors as previously described (33). To generate activated peripheral blood T cells, cells were incubated in complete medium with 10 ng/ml PMA (Sigma-Aldrich) and 1 mM ionomycin (Sigma-Aldrich) for 12 h and then were maintained in complete medium with 100 U/ml IL-2. Activated cells were typically >90% CD3 positive as determined by FACS analysis with mAb OKT3 (American Type Culture Collection).

Construction of VCAM-1 mutants

The following primer sets (obtained from Sigma-Genosys or Seqwright DNA Sequencing) were used to create indicated substitutions and domain deletion (Δ) mutants via Quikchange (Invitrogen Life Technologies) mutagenesis (according to manufacturer's protocol) within IgG2a-tagged 7D-VCAM-1 cloned into pFastBac1: VCAM-1(D40A), 5′(f)-ACCCAGATAGCTAGTCCACTGAA-3′ and 5′(r)-TTCAGTGGACT GTCTATCTGGGT-3′; VCAM-1(D328A), 5′(f)-GAACCCAGATAGC TAGCCCTCTGAG-3′ and 5′(r)-GCTCAGAGGGCTAGCTATCTGCC TTC-3′; VCAM-1ΔD2, 5′(f)-AAATTGGAAAAAGGAAATCCAAG TCTACATATCA-3′ and 5′(r)-TGATATGTAGACTTGGATTCCTTT TTCCAATTT-3′;VCAM-1ΔD3,5′(f)-GCTGTAAAAGAATTGTTTAC TGTTGAGATC-3′ and 5′(r)-GATCTCAACAGTAAACAATTCTTT TACAGC-3′; VCAM-1ΔD4, 5′(f)-GTTCAAGAGAAACCATTCCCTA GAGATCCAGAA-3′ and 5′(r)- TTCTGGATCTCTAGGGAATGGTT TCTCTTAAC-3′; VCAM-1ΔD5, 5′(f)-GTGGAGCTCTACTCATATG TCAATGTTGCC-3′ and 5′(r)-GGCAACATTGACATATGAGTAGA GCTCCAC-3′; VCAM-1ΔD6, 5′(f)-AGTACGCAAACACTTACTCC AAAAGACATA-3′ and 5′(r)-TATGTCTTTTGGAGTAAGTGTTTG CGTACT-3′. Expression and fast protein liquid chromatography purification (AKTAprime; Amersham Biosciences) of IgG2a-tagged VCAM-1 constructs from SF9 supernatant was performed on Protein G-Sepharose. For generation of FLAG epitope-tagged VCAM-1 constructs, the original IgG2a sequence was looped out from the full-length 7D VCAM-1 construct (in pFastBac1) and replaced with the peptide sequence GGGDYNDDDDK (FLAG epitope underlined) by Quikchange mutagenesis. The following primer set was used: 7D VCAM-1 (FLAG) 5′(f)-TATTTTTCTCCTGAGGGAGGAGGAGAT TACAAGGATGATGATGATAAGTAGTGACTCGAGAAGTAC TAG-3′ and 7D VCAM-1 (FLAG) 5′(r)-CTAGTACTTCTCG AGTCACTACTTATCATCATCATCCTTGTAATCTCCTCCTCCCTC AGGAGAAAAATA-3′. To create the alternatively spliced isoform of VCAM-1 (6D VCAM-1 (FLAG)), the fourth domain of the 7D VCAM-1 (FLAG) construct was deleted with the following overlapping primer set: 6D VCAM-1 (FLAG) 5′-GGTGGAATTAATTGTTCAAG CATTCCCTAGAGATCCAGAA-3′ and 6D VCAM-1 (FLAG) 5′-TTCT GGATCTCTAGGGAATGCTTGAACAATTAATTCCACC-3′. FLAG-tagged VCAM-1 proteins were purified on anti-FLAG M2-agarose (Sigma-Aldrich) by fast protein liquid chromatography per the manufacturer's instructions. Purity of VCAM-1 preparations were determined by SDS-PAGE and Coomassie staining.

Soluble VCAM-1 binding assays

For analysis of soluble VCAM-1 binding to integrin $\alpha_4\beta_1$, cells were resuspended at a concentration of 5×10^5/ml in binding buffer (20 mM HEPES (pH 7.4), 12 mM $NaHCO_3$, 150 mM NaCl, 2.5 mM KCl, 1 mg/ml glucose, 1 mg/ml BSA) supplemented with either 1 mM $MgCl_2/CaCl_2$ or 1 mM $MnCl_2$. Indicated VCAM-1 constructs were incubated with cells at various concentrations for 30 min at room temperature (RT). Cells were then washed in binding buffer at 4°C and incubated with appropriate secondary Abs. For IgG2a-tagged VCAM-1 constructs, FITC-conjugated goat anti-mouse Ig (BioSource International) was incubated (2 μg/ml) with cells for 30 min at 4°C, washed, and then analyzed by flow cytometry (Epics XL-MCL; Beckman Coulter). For FLAG-tagged VCAM-1 constructs, either anti-VCAM-1 mAb 1.4C3 (Chemicon International) or anti-FLAG mAb M2 (Sigma-Aldrich) was incubated with VCAM-1 bound cells for 30 min at 4°C. Monoclonal Ab 1.4C3 recognizes both 6D and 7D VCAM-1 to a similar extent (27). Cells were then washed and incubated with FITC-conjugated goat anti-mouse Ab (BioSource International). Bound VCAM-1 was measured by FACS analysis. A minimum of 5000 events were analyzed per sample.

Static cell adhesion assays

Goat anti-mouse IgG2a (Southern Research Associates) or anti-FLAG mAb M2 (Sigma-Aldrich) was immobilized (5 μg/ml) overnight at 4°C in 50 mM Tris-HCl (pH 7.5), 150 mM NaCl (TBS) onto Hi-Bind plates (BD Biosciences). After blocking with 1% BSA in TBS for 1 h at RT, 7D VCAM-1(Ig), 6D VCAM-1(Ig), 7D VCAM-1(FLAG), or 6D VCAM-1(FLAG) was captured at indicated concentrations in TBS for 1 h at RT. During this time, Ramos cells (25×10^6) were resuspended in 1 ml of complete medium and incubated for 1 h at 37°C in the presence of 50 μg/ml calcein-AM (Molecular Probes). After labeling, cells were resuspended at a concentration of 5×10^6/ml in TBS supplemented with 1 mM $MnCl_2$. For experiments involving inhibition of cell adhesion, indicated concentrations of 6D and 7D VCAM-1(FLAG) were preincubated with cells before addition to plates coated with 7D VCAM-1(Ig). Cells (2.5×10^5 in 50 μl) were added to washed plates and incubated for 30 min at 37°C. After incubation, plates were washed three times with TBS/$MnCl_2$. Adherent cells were lysed, and cell adhesion was quantified on an Ultra384 plate reader (Tecan) using 485 and 535 nM excitation and emission filters after cell lysis in 50 mM Tris-HCl (pH 7.5), 1% Nonidet P-40, and 5 mM EDTA.

VCAM-1 ELISA

ELISAs were performed concurrently with cell adhesion assays. 7D VCAM-1(Ig) or 6D VCAM-1(Ig) was immobilized as described above for cell adhesion assays in a separate 96-well plate. After immobilization, plates were incubated for 1 h at RT with biotinylated mAb 1.4C3 (Chemicon International; 1 μg/ml) in TBS supplemented with 0.1% (w/v) BSA (TBS/BSA). After washing three times in TBS/BSA, plates were incubated with streptavidin-HRP (Southern Biotechnology Associates; 1 μg/ml) in TBS/BSA for 30 min at RT. Plates were washed five times, and 3,3′,5,5′ tetramethylbenzidine was added (1-Step Turbo TMB-ELISA; Pierce). After color development, reaction was stopped with 1/1 dilution of 1.5 N H_2SO_4, and absorbance was read at 450 nm.

Parallel plate flow

Goat anti-mouse IgG2a (20 μg/ml in 0.1 M $NaHCO_3$ (pH 9.5)) was immobilized overnight at 4°C onto 24 × 50-mm slides cut from 15 × 100-mm polystyrene petri dishes. The slides were then washed with PBS, and 7D VCAM-1(Ig) or 6D VCAM-1(Ig) was captured at a concentration of 2 nM for attachment assays or 1 nM for detachment assays measuring the strength of cell adhesion. The slides were then blocked with 2% (w/v) BSA for 2 h at RT and assembled into a parallel plate flow chamber. When parallel plate flow chambers were used in detachment assays, Jurkat T cells at 6×10^6 cells/ml in running buffer (10 nM Tris, 103 mM NaCl, 24 mM $NaHCO_3$, 5.5 mM glucose, 5.4 mM KCl, 2 mg/ml BSA (pH 7.4)) were injected into the flow chamber and allowed to settle on the slides for 10 min. Using a computer-controlled syringe pump (Harvard Apparatus), an increasing linear gradient of shear flow was pulled over the adherent cells for 300 s, and the number of adherent cells remaining was recorded by digital microscopy. Shear stress calculations were determined every 20 s, where the sheer stress in dynes/cm^2 was defined as $(6\mu Q)/(wh^2)$, where μ is the viscosity of the medium (0.007), Q is the flow rate in cm^3/s, w is the width of the chamber (0.3175 cm), and h is the height of the chamber (0.01524 cm). When parallel plate flow was used in attachment assays, Jurkat T cells (4×10^6 cells/ml in running buffer) were injected into the chamber at a constant flow rate of 2.85 dynes/cm^2 for 120 s. The number of cells attached was recorded by digital microscopy (VI-470 charge-coupled device (CCD) video camera; Optronics Engineering) at ×20 on an inverted Nikon DIAPHOT-TMD microscope every 10 s and was plotted against time.

Cell spreading assays

Goat anti-mouse IgG2a (Southern Biotechnology Associates) was immobilized (20 μg/ml in 0.1M $NaHCO_3$ (pH 9.5)) overnight at 4°C onto high-binding 96-well plates (Costar). Plates were washed with PBS, incubated with indicated concentrations of 7D VCAM-1(Ig) or 6D VCAM-1(Ig) for 1 h at RT in PBS, and blocked with 1% (w/v) BSA (2 h at RT). Wells were washed with PBS and 3.0×10^4 HPB-ALL T cells in complete medium were added to wells and incubated for 30 min at 37°C. Images of the cells were captured by a VI-470 CCD video camera (Optronics Engineering) using a ×20 objective on a Nikon DIAPHOT-TMD inverted microscope. The images were analyzed using NIH Image 1.58 (available via ⟨ftp://rsbweb.nih.gov/pub/nih-image/⟩), and data are presented as the percentage of cells spreading.

Migration assays

Migration assays were performed in 3-μM pore size Transwells (24-well; Costar). Upper chambers were precoated with goat anti-mouse IgG2a (5 μg/ml) in 50 mM Tris-HCl (pH 7.5), 150 mM NaCl (50 μl) overnight at 4°C. Upper chambers were then blocked with 10% BSA. After blocking, ICAM-1(Ig) (5 μg/ml) was incubated for 1 h at RT. After washing, upper chambers were loaded with Jurkat cells (2×10^5 cells) in 160 μl of medium (RPMI 1640 supplemented with 10% FBS, 100 U/ml penicillin, and 100 μg/ml streptomycin). Lower chambers contained 600 μl of medium supplemented with 15 ng/ml stromal cell-derived factor 1α to induce chemotaxis. In control experiments, the α_4-specific cyclic hexapeptide TBC772 (34) was preincubated with the cells (15 min at RT) at a concentration of 100 μM. To block binding to ICAM-1, the upper wells of Transwells were incubated with anti-ICAM-1 mAb HA58 (20 μg/ml) for 15 min at RT before the addition of Jurkat cells. In tests with soluble VCAM-1 (FLAG tagged), cells were preincubated with indicated concentrations of VCAM-1 construct and then added to the upper chamber of the ICAM-1-coated Transwells. After a 4-h incubation at 37°C, upper chambers were removed and cells in the lower chamber were collected and counted on a hemocytometer. Results are expressed as the total number of cells migrated.

Homotypic aggregation assay

Jurkat cells or α_4-negative Jurkat variant cells were resuspended to 2×10^6 cells in complete medium and then added (200 μl) to 96-well tissue culture plates with indicated concentrations of soluble 6D and 7D VCAM-1(FLAG) constructs or indicated VCAM-1(Ig) constructs. Cells were incubated for 2 h at 37°C, 5% CO_2. For blocking experiments, TBC772 was used at a concentration of 100 μM and added at the same time as the soluble VCAM-1 constructs. Images of cells were captured on an IMT-2 inverted microscope (Olympus) equipped with a SPOT-cooled CCD camera (Diagnostic Instruments). Original magnification was ×20. Qualitative assessment of cellular aggregation was based on the scale presented in Fig. 7*A*. Briefly, random images from wells were scored on a scale between 1 and 5, with 1 representing unstimulated cells and 5 representing maximal aggregation.

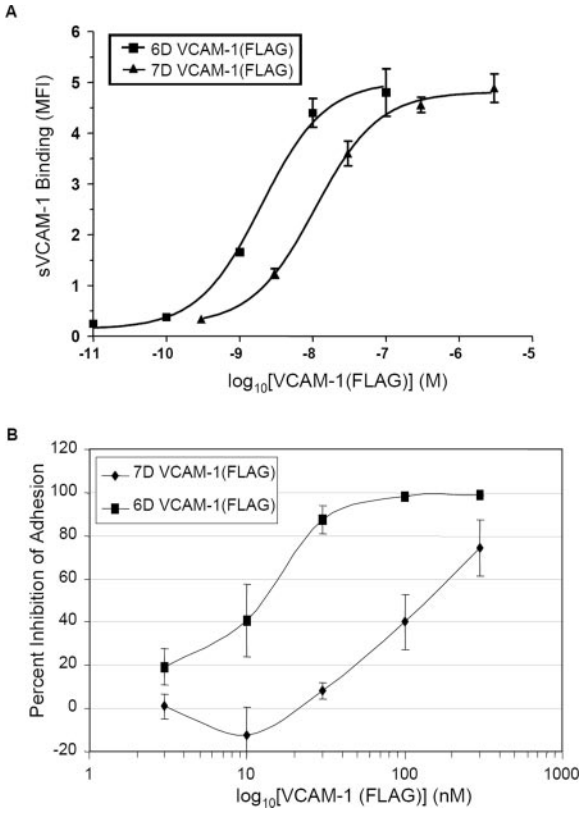

FIGURE 1. Binding of soluble monomeric 6D and 7D VCAM-1(FLAG) to integrin $\alpha_4\beta_1$. *A*, Various concentrations of 6D or 7D VCAM-1(FLAG) were incubated with Jurkat T cells in buffer containing 1 mM $MnCl_2$. After washing, bound VCAM-1 was detected by flow cytometry with primary mAb 1.4C3 (nonfunction-blocking anti-VCAM-1) and secondary FITC-conjugated goat anti-mouse polyclonal Ab. Data are expressed as the mean fluorescence intensity (MFI) calculated from at least 5000 events and represent an average ± SD of four independent experiments. *B*, Soluble monomeric 6D and 7D VCAM-1(FLAG) inhibition of $\alpha_4\beta_1$-dependent cell adhesion to immobilized 7D VCAM-1. Indicated concentrations of monomeric 6D or 7D VCAM-1(FLAG) were preincubated with Ramos cells. Cell adhesion to captured Ig2a-tagged 7D-VCAM-1 was then analyzed. Results represent the mean ± SD of triplicate wells and are expressed as a percent inhibition of maximal cell adhesion. Experiments are representative of two performed.

Results

Alternatively spliced 6D VCAM-1 binds to integrin $\alpha_4\beta_1$ with a higher relative affinity than 7D VCAM-1

Extracellular Ig-like domains 1 and 4 of 7D VCAM-1 can mediate integrin $\alpha_4\beta_1$-dependent cell adhesion (25–27, 29, 30); however, the functional importance of these two domains in regulating soluble VCAM-1 binding to $\alpha_4\beta_1$ has not been examined. To address this, we generated COOH-terminal FLAG-tagged 7D VCAM-1 (7D VCAM-1(FLAG)) and the alternatively spliced 6D VCAM-1 (6D VCAM-1(FLAG)), which lacks domain 4 (14), and tested them for binding to cell surface-expressed $\alpha_4\beta_1$. Unexpectedly, 6D VCAM-1(FLAG) bound with a higher relative affinity to $\alpha_4\beta_1$ on Jurkat cells than did 7D VCAM-1(FLAG) (Fig. 1*A*). This was true in the presence of 1 mM $MnCl_2$ (Fig. 1*A*) or when the binding buffer contained 1 mM $MgCl_2$ and 1 mM $CaCl_2$ (data not shown). The EC_{50} of 6D VCAM-1(FLAG) binding to integrin $\alpha_4\beta_1$ on Jurkat cells in the presence of $MnCl_2$ was 2×10^{-9} M, whereas the EC_{50} of 7D VCAM-1(FLAG) binding under similar conditions was 11×10^{-9} M. Increased binding of 6D VCAM-1(FLAG) was also observed on activated peripheral blood T cells (data not shown). Binding was completely inhibited by the α_4 specific antagonist peptide TBC772 (data not shown).

The relative differences in affinity between 6D VCAM-1(FLAG) and 7D VCAM-1(FLAG) for $\alpha_4\beta_1$ were further compared in experiments designed to determine their ability to inhibit $\alpha_4\beta_1$-dependent cell adhesion. Soluble 6D and 7D VCAM-1(FLAG) were preincubated with Ramos cells in the presence of $MnCl_2$ before adhesion to captured 7D VCAM-1(Ig). In this system, Ramos cell adhesion to immobilized 7D VCAM-1(Ig) was $\alpha_4\beta_1$-dependent based on function blocking Ab studies using mAb HP2/1 (data not shown). 7D VCAM-1(FLAG) inhibited Ramos cell adhesion with an IC_{50} of ~150 nM (Fig. 2*B*). 6D VCAM-1(FLAG) inhibited cell adhesion with an IC_{50} of ~13 nM (Fig. 1*B*), indicating a >10-fold increase in relative affinity of 6D VCAM-1 over 7D VCAM-1 for integrin $\alpha_4\beta_1$.

Ig-like domains 4 through 6 and Asp^{328} negatively regulate soluble VCAM-1 binding to integrin $\alpha_4\beta_1$

To elucidate the residues and domains important for increased soluble 6D VCAM-1 binding to integrin $\alpha_4\beta_1$, a variety of amino acid

substitutions and domain deletions within IgG2a-tagged VCAM-1 were generated (represented schematically in Fig. 2*A*) and compared for soluble binding to $\alpha_4\beta_1$. Protein purity was verified by SDS-PAGE and Coomassie staining (Fig. 2*B*). Briefly, aspartic acid to alanine substitutions were made in the reported $\alpha_4\beta_1$ binding domains (D40 and D328) either singly or dually in full-length VCAM-1 (designated VCAM-1(D40A), VCAM-1(D328A), or VCAM-1(D40,328A)). Deletions of Ig-like domains were also conducted including the second (VCAM-1ΔD2), third (VCAM-1ΔD3), fourth (referred to here as 6D VCAM-1(Ig)), fifth (VCAM-1ΔD5), and sixth (VCAM-1ΔD6) domain.

Removal of domains 2 or 3 of full-length VCAM-1 did not affect soluble VCAM-1 binding (Fig. 2*C*); however, similar to the 6D VCAM-1(FLAG), removal of the 4th Ig-like domain in this Ig2a-tagged construct (referred to as 6D VCAM-1(Ig)) resulted in increased soluble VCAM-1 binding to Jurkat cells over wild-type 7D VCAM-1(Ig). Likewise, removal of domain 5 or 6 gave similar increased binding. A single amino acid substitution within domain 4 (D328A) demonstrated increased $\alpha_4\beta_1$-dependent binding. No binding of either the single substitution (D40A), or the double substitution mutant (D40,328A) was detected. All constructs were tested at a concentration of 30 nM in the presence of 1 mM $MnCl_2$. In the presence of 1 mM $MgCl_2$ and $CaCl_2$, removal of domain 4 or substitution of Asp^{328} with Ala resulted in a similar increase in soluble VCAM-1 binding (data not shown). Significant binding of 2D VCAM-1(Ig), a construct containing only the two NH_2-terminal domains of VCAM-1 tagged with the Fc region of IgG2a, was only observed in the presence of 1 mM $MnCl_2$ (data not shown). In summary, Asp^{40} is essential for soluble VCAM-1 binding, and Asp^{328} substitution with alanine or removal of the fourth, fifth, or sixth Ig-like domain increases soluble VCAM-1 binding to integrin $\alpha_4\beta_1$.

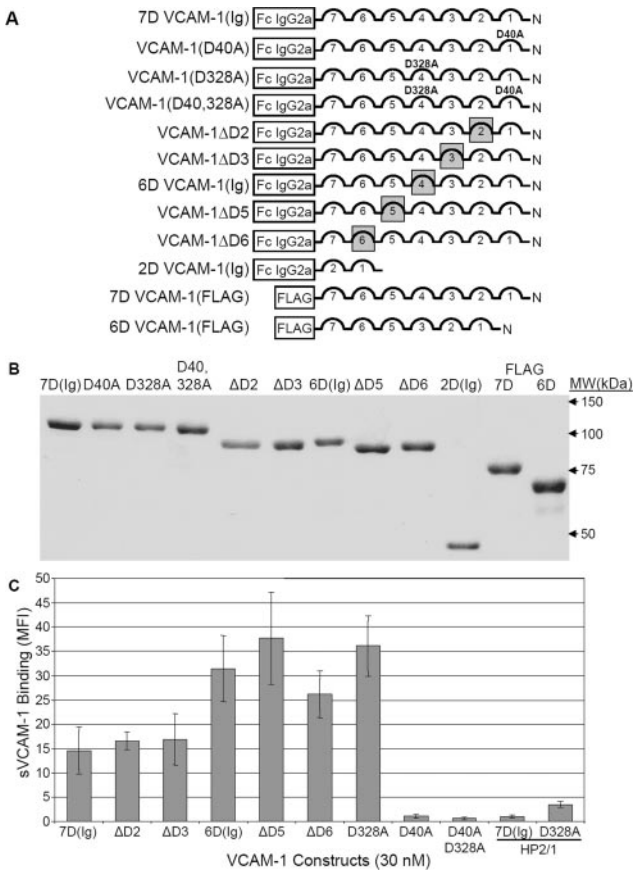

FIGURE 2. Structure/function analysis of soluble VCAM-1 binding to integrin $\alpha_4\beta_1$. *A*, Schematic representation of purified VCAM-1 constructs generated. Constructs contain either a FLAG tag or mouse IgG2a Fc region on the C terminus. Deleted domains are shaded. *B*, SDS-PAGE analysis of purified VCAM-1 constructs. Baculovirus-expressed IgG2a-tagged constructs were purified on protein-G Sepharose columns, and FLAG-tagged VCAM-1 constructs were purified on anti-FLAG Sepharose columns. Proteins were separated by SDS-PAGE (10%) under reducing conditions and visualized with Coomassie blue staining. *C*, Soluble VCAM-1 binding to Jurkat cells. Jurkat cells were incubated with various Ig-tagged soluble VCAM-1 constructs at 30 nM in the presence of 1 mM $MnCl_2$. After washing, bound VCAM-1 was detected with FITC-conjugated goat anti-mouse IgG2a. For blocking experiments, mAb HP2/1 (IgG1 isotype) was preincubated with Jurkat cells before the addition of soluble VCAM-1. Data are expressed as the average MFI ± SD from three separate experiments. MFIs were calculated from at least 5000 events.

Increased strength of adhesion to 7D VCAM-1 under conditions of flow

Adhesion assays were performed on both Ig-tagged and FLAG-tagged VCAM-1 constructs to verify the role played by VCAM-1 domain 4 in static cell adhesion assays. We observed very little difference in the EC_{50} of binding to VCAM-1 constructs with or without this domain (Fig. 3). From two experiments, the EC_{50} range of cell adhesion for 7D VCAM-1(Ig) was $50–56 \times 10^{-12}$ M, and the EC_{50} of cell adhesion for 6D VCAM-1(Ig) was $50–62 \times 10^{-12}$ M. Equal capture of VCAM-1 was confirmed by ELISA with biotinylated VCAM-1 mAb 1.4C3 (Fig. 3, dotted line), which recognizes an epitope within domain 2 of VCAM-1 in both 7D and 6D VCAM-1 (27). No significant adhesion was seen to control wells coated with BSA (data not shown). Similar results were obtained when FLAG-tagged 6D and 7D VCAM-1 were captured with anti-FLAG Ab M2, where the range in EC_{50} for Ramos cell adhesion to 7D VCAM-1(FLAG) was $100–140 \times 10^{-12}$ M, and to 6DVCAM-1(FLAG) it was $90–110 \times 10^{-12}$ M (data not shown)

Experiments were then performed to measure the rates of attachment and strength of adhesion of Jurkat cells to 7D VCAM-1(Ig) and 6D VCAM-1(Ig). In Fig. 4*A*, VCAM-1 constructs were captured onto plastic immobilized goat anti-mouse IgG2a. Jurkat cells were perfused over the substrates in a parallel plate flow chamber at a flow rate of 0.3 ml/min (2.8 dynes/cm^2), and cell adhesion was quantified from images captured every 20 s. Although the rate of adhesion to 6D VCAM-1(Ig) was consistently

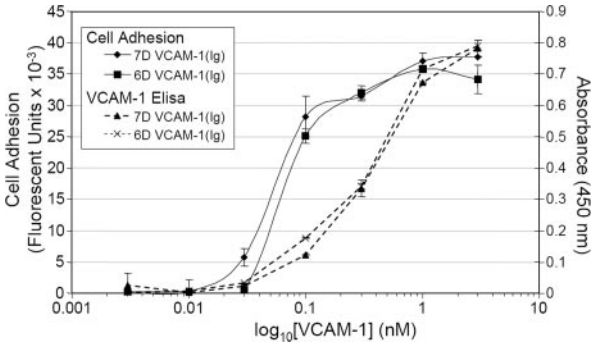

FIGURE 3. Static Ramos cell adhesion to VCAM-1. *A*, Cell adhesion assays were performed as described in *Materials and Methods* in the presence of 1 mM $MnCl_2$. 7D VCAM-1(Ig) and 6D VCAM-1(Ig) were captured at indicated concentrations. In a parallel 96-well plate that was coated with similar concentrations of VCAM-1, an ELISA was performed to measure the amount of captured VCAM-1. Primary anti-VCAM-1 mAb used was biotinylated 1.4C3. Ab binding was detected with streptavidin-HRP. Data are expressed as average ± SD from triplicate determinations.

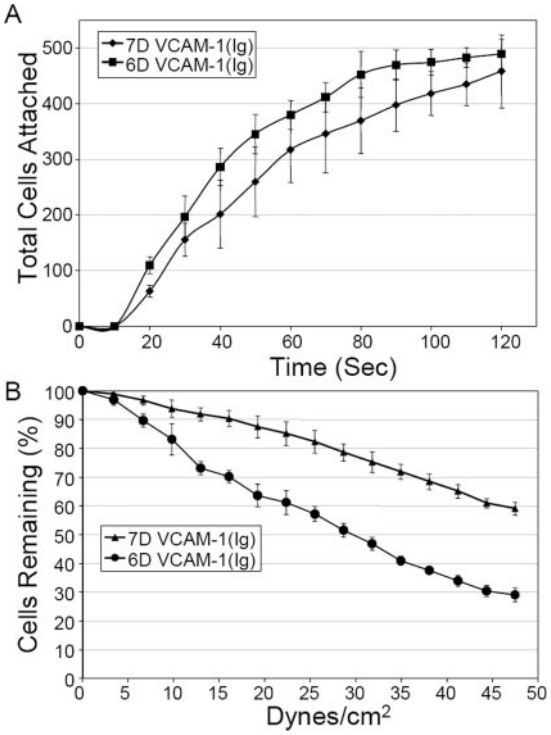

FIGURE 4. Increased resistance to shear force of cells on 7D VCAM-1. *A*, Assessment of Jurkat cell attachment in parallel plate flow. 7D VCAM-1(Ig) and 6D VCAM-1(Ig) were captured (2 nM) with anti-IgG2a Ab immobilized at 5 μg/ml in flow chambers. Jurkat cells were perfused over the substrates at a flow rate of 0.3 ml/min (2.8 dynes/cm^2) and adherent cells were enumerated every 20 s. Results are expressed as the mean number of cells attached ± SD from triplicate runs. *B*, Jurkat cell detachment assays under conditions of flow. 7D VCAM-1(Ig) and 6D VCAM-1(Ig) were captured (1 nM) with anti-IgG2a Ab immobilized at 5 μg/ml in flow chambers. Jurkat cells were perfused over the substrate and then flow was stopped. After a 10-min incubation period to allow cell adhesion, flow was initiated and a linear gradient of shear was applied. Cells were enumerated as described in *A*, and data are expressed as the mean percentage of cells remaining ± SD from triplicate runs.

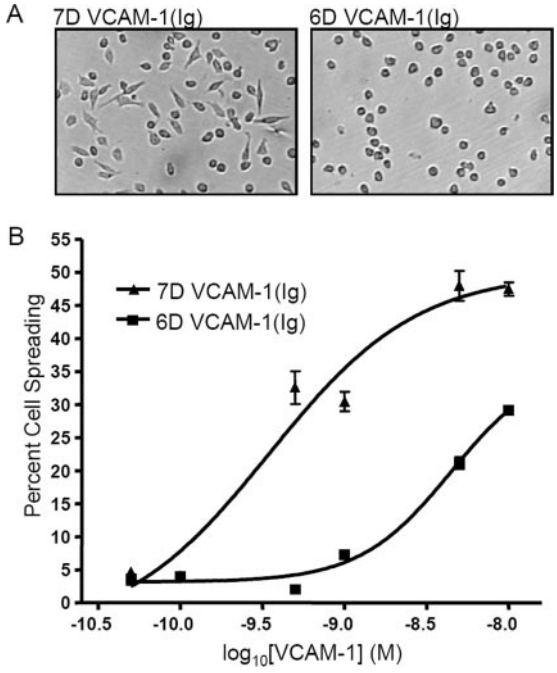

FIGURE 5. Increased cell spreading on 7D VCAM-1. *A*, HPB-ALL cell spreading on 7D VCAM-1(Ig) and 6D VCAM-1(Ig). Cell spreading assays were performed as described in *Materials and Methods*. 7D VCAM-1(Ig) and 6D VCAM-1(Ig) were captured onto immobilized anti-IgG2a at a concentration of 0.5 nM. HPB-ALL cells were incubated on the substrate for 30 min. One of three representative experiments is shown (initial magnification, ×200). *B*, Dose-dependent spreading of HPB-ALL cells on VCAM-1. VCAM-1 constructs were captured as described in *A* at indicated concentrations. Images were captured after a 30-min incubation, and results are expressed as the mean percentage of cells spreading ± SD from three experiments.

higher than to 7D VCAM-1, this difference did not appear significant. The cells immediately adhered to the 6D and 7D VCAM-1 substrates, as no cell rolling was detected. No adhesion was observed to immobilized BSA in control chambers (data not shown). In Fig. 4*B*, Jurkat cells were perfused over substrate, then flow was stopped and cells were allowed to adhere for 10 min. Flow was then initiated, and cell adhesion was quantified as shear stress was increased. Under these conditions, cells adhered more avidly to full-length 7D VCAM-1(Ig) than to 6D VCAM-1(Ig) (Fig. 4*B*). Cells also adhered more avidly to 7D VCAM-1(Ig) than to VCAM-1(D328A) immobilized at similar concentrations (data not shown)

Increased cell spreading on 7D VCAM-1

Immobilized 7D VCAM-1(Ig) was also more potent than immobilized 6D VCAM-1(Ig) in inducing cell spreading. HPB-ALL cells were used in these assays because $\alpha_4\beta_1$-dependent shape changes are more readily quantified with this cell type (35). Very little spreading occurred on 6D VCAM-1(Ig) that was captured at a concentration of 0.5 nM, whereas cell spreading is clearly seen on 7D VCAM-1(Ig) when coated at an identical concentration (Fig. 5*A*). 6D VCAM-1(Ig) could induce cell spreading at coating concentrations greater than 1 nM; however, significantly less 7D VCAM-1(Ig) was required to induce cell spreading of HPB-ALL cells (Fig. 5*B*). Thus, even though there is very little difference in static cell adhesion of cells to the different VCAM-1 constructs, the strength of adhesion of cells at high shear forces and the ability to support cell spreading is greater with 7D VCAM-1(Ig) than with 6D VCAM-1(Ig).

Soluble 6D VCAM-1 induces cell migration on the $\alpha_L\beta_2$ substrate ICAM-1

7D VCAM-1 signaling through integrin $\alpha_4\beta_1$ can induce Jurkat cell locomotion on the $\alpha_L\beta_2$ substrate ICAM-1 (24). To determine whether soluble 6D VCAM-1 could promote $\alpha_L\beta_2$-dependent migration, cell migration assays on ICAM-1-coated Transwells were performed. As ICAM-1 was captured through its IgG2a COOH-terminal tag, FLAG-tagged VCAM-1 constructs were used to prevent their binding to the capture Ab. Stromal cell-derived factor 1α was used in the lower chambers of the Transwells to induce Jurkat chemotaxis, and 6D VCAM-1(FLAG) (100 nM) was added to the upper chamber of Jurkat cells (2×10^5 cells). As seen in Fig. 6 6D VCAM-1(FLAG) augmented Jurkat chemotaxis on the $\alpha_L\beta_2$ substrate ICAM-1. The $\alpha_4\beta_1$ antagonist peptide TBC772 (34) did not affect basal migration of cells on ICAM-1; however, it did inhibit 6D VCAM-1(FLAG)-induced migration. Monoclonal Ab HA58, a function-blocking anti-ICAM-1 mAb (36), consistently inhibited Jurkat cell migration to basal levels (Fig. 6), which was similar to that seen on BSA-coated Transwells (data not shown). Thus, 6D VCAM-1 can augment $\alpha_L\beta_2$-dependent cellular locomotion on ICAM-1.

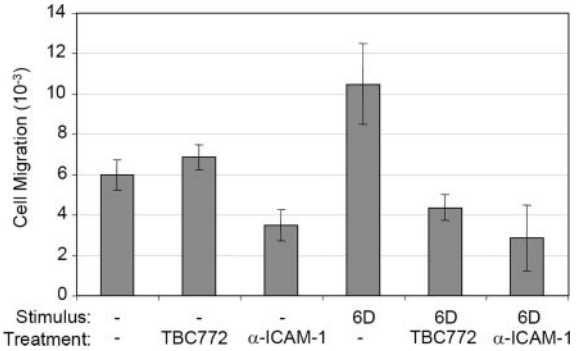

FIGURE 6. 6D VCAM-1-induced migration of Jurkat cells on $\alpha_L\beta_2$ substrate ICAM-1. Jurkat cells were either unstimulated or stimulated with soluble 6D VCAM-1(FLAG) (100 nM) before placement in the upper chamber of ICAM-1-coated Transwells. In control experiments, a cyclic peptide antagonist of $\alpha_4\beta_1$ (TBC772) was preincubated with Jurkat cells for 15 min at RT before the addition of 6D VCAM-1(FLAG) and placement into the upper chambers. For anti-ICAM-1 treatment, upper Transwell chambers were preincubated with mAb HA58 (20 μg/ml) for 15 min before the addition of Jurkat cells. Cells migrating through the Transwells into the lower chamber were collected and enumerated with a hemocytometer. Results are presented as the mean ± SE of the total number of migrated cells from duplicate Transwells. Data are representative of three experiments performed.

Soluble VCAM-1 induces cellular homotypic aggregation

When performing migration assays, cellular aggregation was observed in soluble VCAM-1-treated cells that were incubated on control Transwells coated with BSA (data not shown). Further analysis demonstrated that dose-dependent aggregation of Jurkat cells occurred upon the addition of 6D VCAM-1(FLAG), with maximal aggregation occurring at 30 nM (Fig. 7*B*). 7D VCAM-1(FLAG) also induced homotypic aggregation of Jurkat cells (Fig. 7*B*). VCAM-1-induced aggregation was $\alpha_4\beta_1$ dependent, as TBC772 completely inhibited aggregation (Fig. 7*C*). Likewise, Jurkat cells mutagenized and selected for loss of integrin $\alpha_4\beta_1$ expression (32) did not aggregate upon the addition of soluble 6D VCAM-1(FLAG) (Fig. 7*D*). Analysis of the dimeric Ig-tagged wild-type and mutant VCAM-1 constructs demonstrated a pattern of induction of homotypic aggregation (Fig. 7*E*) that was similar to their extent of measured binding in soluble VCAM-1 binding assays (Fig. 2). Thus, both 6D and 7D VCAM-1, in monomeric or dimeric form, can induce $\alpha_4\beta_1$-dependent cellular homotypic aggregation.

Discussion

Although VCAM-1 can support $\alpha_4\beta_1$-dependent cell adhesion through two of its Ig-like domains, domains 1 and 4 (25–27, 29, 30), the role of these domains in the regulation of soluble VCAM-1 binding to integrin $\alpha_4\beta_1$ has not been addressed. In the present study, we report that the alternatively spliced isoform of VCAM-1, which is generated by the removal of domain 4 (termed 6D VCAM-1), results in an unexpected increase in the apparent affinity of soluble VCAM-1 for $\alpha_4\beta_1$. This was observed in ligand binding assays and in the inhibition of $\alpha_4\beta_1$-dependent cell adhesion. Soluble 6D VCAM-1 was also an efficient agonist of $\alpha_4\beta_1$-dependent functions such as induced cellular migration and homotypic aggregation. When acting as an adhesive substrate, however, domain 4 of full-length VCAM-1 (7D VCAM-1) was required to promote cell spreading and increased resistance to shear force. These results suggest that 6D VCAM-1 and 7D VCAM-1 may play different roles in vivo when present either in solution or as a cell surface-expressed adhesive substrate.

As measured by flow cytometry, the integrin $\alpha_4\beta_1$ binds 7D VCAM-1 with an EC_{50} of $\sim 11 \times 10^{-9}$ M in the presence of 1 mM $MnCl_2$. This is similar to that previously reported for high-affinity interactions between $\alpha_4\beta_1$ and 7D VCAM-1 (EC_{50} of ~50 nM (31)). Under similar conditions, however, 6D VCAM-1 bound integrin $\alpha_4\beta_1$ with a >5-fold increase in apparent affinity (EC_{50} of 2×10^{-9}M) compared with 7D VCAM-1. These results were not due to the use of monomeric FLAG-tagged VCAM-1 constructs, as increased binding of dimeric Ig-tagged 6D VCAM-1 was also observed (Fig. 2*C*). It is not known whether in vivo circulating VCAM-1 is a monomer or dimer. Although other cell adhesion receptors of the Ig family that bind integrins, such as the $\alpha_L\beta_2$ ligand ICAM-1 and $\alpha_4\beta_7$ ligand mucosal addressin cell adhesion molecule-1, can be found on the cell surface or in solution as dimers or oligomers (37, 38), recent studies indicate that in vitro-expressed 7D VCAM-1 is monomeric (39). Regardless, we demonstrate here that either as a monomer or as an Ig-tagged dimer, 6D VCAM-1 binds integrin $\alpha_4\beta_1$ with a higher relative affinity than does 7D VCAM-1. Furthermore, this increased binding was observed on a variety of different lymphocyte cell lines and on activated peripheral blood T cells.

The mechanism by which soluble 6D VCAM-1 binds integrin $\alpha_4\beta_1$ with higher relative affinity than does 7D VCAM-1 is undetermined. We demonstrate here that Asp^{40} within domain 1 of VCAM-1 is essential for soluble VCAM-1 binding. Also, removal of Ig-like domains COOH-terminal to domain 3 or simply substituting Asp^{328} with Ala increases the relative affinity of 7D VCAM-1 for $\alpha_4\beta_1$. Previous functional and structural studies of the two NH_2-terminal domains of VCAM-1 (domains 1 and 2) have demonstrated that the primary $\alpha_4\beta_1$ binding site in domain 1 resides in a solvent-exposed loop (the C-D loop, which contains the essential residue Asp^{40}) (25, 27, 29, 40, 41). A secondary "synergy" site, the C′-E loop-E strand, is located in the upper face of domain 2 (30), spatially close to the C-D loop of domain 1 (40, 41). This mechanism of $\alpha_4\beta_1$ binding VCAM-1 domains 1 and 2 may be similar to integrin $\alpha_5\beta_1$ binding fibronectin. In this case, $\alpha_5\beta_1$ binds to a primary "RGD" loop in the fibronectin type III repeat 10 and to a synergy site centered around the "PHSRN" loop in fibronectin type III repeat 9 (42). By introducing interdomain disulfide bonds at the interface between fibronectin type III repeats 9 and 10, Altroff et al. (43) have recently shown that maintaining a 28° angle of tilt between these domains results in higher-affinity interactions with integrin $\alpha_5\beta_1$. The crystal structures of VCAM-1 domains 1 and 2 demonstrate that the relative orientation of the two domains is not fixed (40, 41) and that there is a high degree of flexibility (ranging from 7.3–39.9° from five different crystal monomers) in the two-dimensional angle of tilt between the two domains (44). Perhaps removal of Ig-like domains COOH-terminal to domain 3 or merely substituting Asp^{328} with Ala results in a subtle conformational change that maintains the angle between domains 1 and 2 such that the domain 1 C-D loop and domain 2 C′-E loop-E strand synergy site present an optimal integrin $\alpha_4\beta_1$ binding topology. Indeed, the overall structure of 7D VCAM-1 is dependent on COOH-terminal regions. For example, an endoproteinase Glu-C cleavage site between domain 3 and domain 4 of 7D VCAM-1 is no longer sensitive to proteolysis upon removal of domains 5–7 (45). Furthermore, deletion of domain 4 in 7D VCAM-1 decreases binding of the domain 1-specific mAb 4B9 (27). Mutational studies, including substitution of residues within the domain 2 synergy site (28) in 6D VCAM-1, will begin to address the mechanism of increased 6D VCAM-1 affinity for integrin $\alpha_4\beta_1$. Also, it will be interesting to determine whether 6D VCAM-1 has a higher relative affinity for other VCAM-1 binding

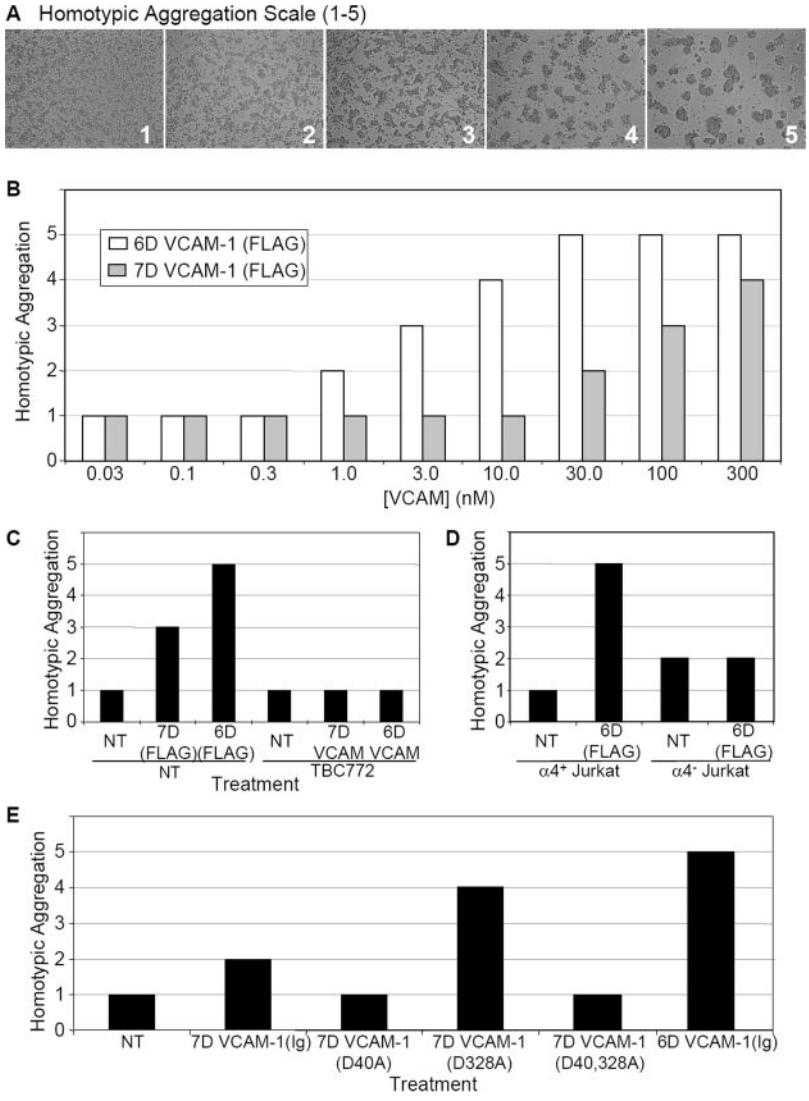

FIGURE 7. Homotypic cellular aggregation induced by soluble VCAM-1. *A*, Jurkat cells were treated with various concentrations of VCAM-1 and scored for homotypic aggregation. The aggregation scale ranged from 1 (untreated, basal aggregation of cells as demonstrated in the *left panel* of *A*) to a maximal aggregation of 5 (*A*, *right panel*). *B*, Various doses of soluble VCAM-1 (6D and 7D-FLAG) were tested for their induction of homotypic aggregation. Results are from one representative experiment of three performed. *C*, VCAM-1(FLAG)-induced (100 nM) homotypic aggregation was inhibited by the $\alpha_4\beta_1$ cyclic peptide antagonist TBC772 (100 μM). Results are representative of three experiments performed. *D*, α_4 null (α_4^-) Jurkat cells were incubated with 6D VCAM-1(FLAG) (30 nM) and homotypic aggregation was scored as in *A*. Results are representative of two experiments performed. *E*, Indicated Ig-tagged VCAM-1 constructs (all used at 100 nM) were tested for their ability to induce homotypic aggregation in Jurkat cells. Aggregation was scored as in *A*. Results are representative of three experiments performed.

integrins such as $\alpha_4\beta_7$ and $\alpha_9\beta_1$, as domain 2 of VCAM-1 has been implicated in integrin selectivity (30).

Even though 6D VCAM-1 has a higher relative affinity for $\alpha_4\beta_1$ in solution, the strength of adhesion of $\alpha_4\beta_1$-bearing cells to 7D VCAM-1 is greater under shear, as seen in parallel plate flow chamber experiments. Increased resistance to shear when cells are adherent to 7D VCAM-1 is likely due to postreceptor occupancy events such as changes in cellular morphology, as cells plated on 7D VCAM-1 flattened out and spread to a greater extent than those plated on equivalent concentrations of 6D VCAM-1 (Fig. 5*A*). However, when 6D VCAM-1 was immobilized at higher densities (e.g., >1 nM coating concentration), cell spreading occurred (Fig 5*B*) and there was little difference in the strength of cell adhesion (data not shown). This demonstrated that 6D VCAM-1 was capable of inducing cell spreading, and that domain 4 of 7D VCAM-1 was not required. Under these conditions, cell shape change was likely a function of ligand density, as the combination of Ig domains 1 and 4 of 7D VCAM-1 renders it bivalent and promotes cell spreading at lower coating concentrations compared with monovalent 6D VCAM-1.

Previous studies have demonstrated that triggering the integrin $\alpha_4\beta_1$ with soluble 7D VCAM-1 can induce cell locomotion (24). In the present study, we show that domain 4 in 7D VCAM-1 is not necessary for this response and that monomeric 6D VCAM-1 can also induce cell migration on ICAM-1. Furthermore, we now demonstrate that soluble VCAM-1 binding to integrin $\alpha_4\beta_1$ on Jurkat cells induces cellular homotypic aggregation. To our knowledge, this is the first demonstration of aggregation induced by a naturally occurring $\alpha_4\beta_1$ ligand, as previous studies have relied on the use of Abs specific for certain epitopes on the integrin α_4 or β_1 chain (46–48). Interestingly, TBC772, an α_4-specific cyclic peptide antagonist (34) thought to mimic the C-D loop from domain 1 of VCAM-1 (49), did not induce aggregation or promote cellular locomotion. This suggests that other regions outside the C-D loop of domain 1 in VCAM-1 can mediate this effect. Thus, by binding soluble 6D or 7D VCAM-1, $\alpha_4\beta_1$ can act as an agonist receptor regulating cellular functions such as cell migration and homotypic aggregation, which could have important physiologic consequences.

In diseases involving inflammation, it is unclear whether soluble VCAM-1 participates in disease progression, down-regulates the severity of disease, or is simply a byproduct of increased proteolytic activity in inflammatory sites. Circulating VCAM-1 in rheumatoid arthritis (17), multiple sclerosis (18), or systemic lupus erythematosis (17) may facilitate leukocyte transendothelial migration by stimulating cell migration on the $\alpha_L\beta_2$ integrin ligand ICAM-1, or it may act as a chemotactic agent (22). By inducing cellular aggregation, soluble VCAM-1 could also retain inflammatory cells at specific sites, for instance, B16 melanoma cells

overexpressing $\alpha_4\beta_1$ aggregate in an $\alpha_4\beta_1$-dependent manner, which prevents spontaneous metastasis after s.c. injection (50). In contrast with inflammation-promoting effects, high concentrations of soluble VCAM-1 could be anti-inflammatory by functioning as a competitive antagonist of $\alpha_4\beta_1$. It will be important to determine the role of soluble VCAM-1 in inflammation, as it could have different effects on disease progression or resolution depending on the stage of inflammation and the cellular source from which it is generated. It will also be of interest to determine the relative levels of 7D VCAM-1 and 6D VCAM-1 that can be found in the circulation in different disease states.

Soluble VCAM-1 may also play a more systemic role in diseases such as sickle cell anemia. For instance, sickle RBCs and premature erythrocytes (reticulocytes) express integrin $\alpha_4\beta_1$ (51, 52), which may play a role in vaso-occlusive events (53, 54) by binding VCAM-1 on endothelial cells (51, 55). Enhanced levels of circulating VCAM-1 have been reported in this disease, with peak concentrations correlating with vaso-occlusive crisis (19). It will be interesting to determine whether soluble VCAM-1 can induce aggregation of sickle RBCs or reticulocytes, as this could be a contributing factor in vaso-occlusion.

In the present study, we provide evidence that the domain 4 of 7D VCAM-1 plays contrasting roles in VCAM-1 function. In solution, domain 4 acts as a negative regulator of soluble VCAM-1 binding to the integrin $\alpha_4\beta_1$, as 6D VCAM-1 binds $\alpha_4\beta_1$ with a higher relative affinity than does 7D VCAM-1. As an immobilized ligand, however, 6D VCAM-1 is not as efficient in inducing cell spreading and resisting shear force as 7D VCAM-1. These results suggest that the relative in vivo importance of 6D VCAM-1 may lie in its role as a soluble agonist rather than an adhesive substrate expressed on the cell surface. Given the potential role for soluble VCAM-1 in a number of diseases, it will be interesting to determine whether there is tissue-specific alternative splicing of VCAM-1, the ratio of circulating 6D VCAM-1 compared with 7D VCAM-1 under different disease conditions, and the structural mechanisms underlying the higher relative affinity of soluble 6D VCAM-1 for integrin $\alpha_4\beta_1$.

Acknowledgments

We thank Dr. A. Rege for critical review of the manuscript and Dr. D. M. Rose for providing Jurkat α_4^- cells.

Disclosures

The authors have no financial conflict of interest.

References

1. Osborn, L., C. Hession, R. Tizard, C. Vassallo, S. Luhowskyj, G. Chi-Rosso, and R. Lobb. 1989. Direct expression cloning of vascular cell adhesion molecule 1, a cytokine-induced endothelial protein that binds to lymphocytes. *Cell* 59: 1203–1211.
2. Gao, J. X., and A. C. Issekutz. 1996. Expression of VCAM-1 and VLA-4 dependent T-lymphocyte adhesion to dermal fibroblasts stimulated with proinflammatory cytokines. *Immunology* 89: 375–383.
3. Morales-Ducret, J., E. Wayner, M. J. Elices, J. M. Alvaro-Gracia, N. J. Zvaifler, and G. S. Firestein. 1992. α_4/β_1 integrin (VLA-4) ligands in arthritis: vascular cell adhesion molecule-1 expression in synovium and on fibroblast-like synoviocytes. *J. Immunol.* 149: 1424–1431.
4. Borrello, M. A., and R. P. Phipps. 1996. Differential Thy-1 expression by splenic fibroblasts defines functionally distinct subsets. *Cell. Immunol.* 173: 198–206.
5. Koopman, G., H. K. Parmentier, W. Schuurman, W. Newman, Y. Shimizu, G. A. VanSeventer, C. deGroot, and S. T. Pals. 1991. Adhesion of human B-cells to follicular dendritic cells involves both lymphocyte function-associated antigen-1/intercellular adhesion molecule 1 and very late activation antigen 4/vascular cell adhesion molecule 1 pathways. *J. Exp. Med.* 173: 1297–1304.
6. Miyake, K., K. Medina, K. Ishihara, M. Kimoto, R. Auerbach, and P. W. Kincade. 1991. A VCAM-like adhesion molecule on murine bone marrow stromal cells mediates binding of lymphocyte precursors in culture. *J. Cell Biol.* 114: 557–565.
7. Salomon, D., L. Crisa, C. F. Mojcik, J. K. Ishii, F. G. Klier, and E. M. Shevach. 1997. Vascular cell adhesion molecule-1 is expressed by cortical thymic epithelial cells and mediates thymocyte adhesion: implications for function VLA4 integrin in T-cell development. *Blood* 89: 2461–2471.
8. Butcher, E. C., and L. J. Picker. 1996. Lymphocyte homing and homeostasis. *Science* 272: 60–66.
9. Springer, T. A. 1994. Traffic signals for lymphocyte recirculation and leukocyte emigration: the multistep paradigm. *Cell* 76: 301–314.
10. Lu, T. T., and J. G. Cyster. 2002. Integrin-mediated long-term B cell retention in the splenic marginal zone. *Science* 297: 409–412.
11. van Seventer, G. A., W. Newman, Y. Shimizu, T. B. Nutman, Y. Tanaka, K. J. Horgan, T. V. Gopal, E. Ennis, D. O'Sullivan, H. Grey, et al. 1991. Analysis of T cell stimulation by superantigen plus major histocompatibility complex class II molecules or by CD3 monoclonal antibody: costimulation by purified adhesion ligands VCAM-1, ICAM-1, but not ELAM-1. *J. Exp. Med.* 174: 901–913.
12. McGilvray, I. D., Z. Lu, R. Bitar, A. P. Dackiw, C. J. Davreux, and O. D. Rotstein. 1997. VLA-4 integrin cross-linking on human monocytic THP-1 cells induces tissue factor expression by a mechanism involving mitogen-activated protein kinase. *J. Biol. Chem.* 272: 10287–10294.
13. Elices, M. J., L. Osborn, Y. Takada, C. Crouse, S. Luhowsky, M. E. Hemler, and R. R. Lobb. 1990. VCAM-1 on activated endothelium interacts with the leukocyte integrin VLA-4/Fibronectin binding site. *Cell* 60: 577–584.
14. Hession, C., R. Tizard, C. Vassallo, S. B. Schiffer, D. Goff, P. Moy, G. Chi-Rosso, S. Luhowskyj, R. Lobb, and L. Osborn. 1991. Cloning of an alternate form of vascular cell adhesion molecule-1 (VCAM1). *J. Biol. Chem.* 266: 6682–6685.
15. Levesque, J. P., Y. Takamatsu, S. K. Nilsson, D. N. Haylock, and P. J. Simmons. 2001. Vascular cell adhesion molecule-1 (CD106) is cleaved by neutrophil proteases in the bone marrow following hematopoietic progenitor cell mobilization by granulocyte colony-stimulating factor. *Blood* 98: 1289–1297.
16. Garton, K. J., P. J. Gough, J. Philalay, P. T. Wille, C. P. Blobel, R. H. Whitehead, P. J. Dempsey, and E. W. Raines. 2003. Stimulated shedding of vascular cell adhesion molecule 1 (VCAM-1) is mediated by tumor necrosis factor-α-converting enzyme (ADAM 17). *J. Biol. Chem.* 278: 37459–37464.
17. Wellicome, S. M., P. Kapahi, J. C. Mason, Y. Lebranchu, H. Yarwood, and D. O. Haskard. 1993. Detection of a circulating form of vascular cell adhesion molecule-1: raised levels in rheumatoid arthritis and systemic lupus erythematosus. *Clin. Exp. Immunol.* 92: 412–418.
18. Matsuda, M., N. Tsukada, K. Miyagi, and N. Yanagisawa. 1995. Increased levels of soluble vascular cell adhesion molecule-1 (VCAM-1) in the cerebrospinal fluid and sera of patients with multiple sclerosis and human T lymphotropic virus type-1-associated myelopathy. *J. Neuroimmunol.* 59: 35–40.
19. Duits, A. J., R. C. Pieters, A. W. Saleh, E. van Rosmalen, H. Katerberg, K. Berend, and R. A. Rojer. 1996. Enhanced levels of soluble VCAM-1 in sickle cell patients and their specific increment during vasoocclusive crisis. *Clin. Immunol. Immunopathol.* 81: 96–98.
20. Kitani, A., N. Nakashima, T. Matsuda, B. Xu, S. Yu, T. Nakamura, and T. Matsuyama. 1996. T cells bound by vascular cell adhesion molecule-1/CD106 in synovial fluid in rheumatoid arthritis: inhibitor role of soluble vascular cell adhesion molecule-1 in T-cell activation. *J. Immunol.* 156: 2300–2308.
21. Kitani, A., N. Nakashima, T. Izumihara, M. Inagaki, X. Baoui, S. Yu, T. Matsuda, and T. Matsuyama. 1998. Soluble VCAM-1 induces chemotaxis of Jurkat and synovial fluid cells bearing high affinity very late antigen-4. *J. Immunol.* 161: 4931–4938.
22. Tokuhira, M., S. Hosaka, M. V. Volin, G. K. Haines, III, K. J. Katschke, Jr., S. Kim, and A. E. Koch. 2000. Soluble vascular cell adhesion molecule 1 mediation of monocyte chemotaxis in rheumatoid arthritis. *Arthritis Rheum.* 43: 1122–1133.
23. Koch, A. E., M. M. Halloran, C. J. Haskell, M. R. Shah, and P. J. Polverini. 199. Angiogenesis mediated by soluble forms of E-selectin and vascular cell adhesion molecule-1. *Nature* 376: 517–519.
24. Rose, D. M., V. Grabovsky, R. Alon, and M. H. Ginsberg. 2001. The affinity of integrin $\alpha_4\beta_1$ governs lymphocyte migration. *J. Immunol.* 167: 2824–2830.
25. Osborn, L., C. Vassallo, B. G. Browning, R. Tizard, D. O. Haskard, C. D. Benjamin, I. Dougas, and T. Kirchhausen. 1994. Arrangement of domains, and amino acid residues required for binding of vascular cell adhesion molecule-1 to its counter-receptor VLA-4 ($\alpha_4\beta_1$). *J. Cell Biol.* 124: 601–608.
26. Vonderheide, R. H., and T. A. Springer. 1992. Lymphocyte adhesion through very late antigen 4: evidence for a novel binding site in the alternatively spliced domain of vascular cell adhesion molecule 1 and an additional α_4 integrin counter-receptor on stimulated endothelium. *J. Exp. Med.* 175: 1433–1442.
27. Vonderheide, R. H., T. F. Tedder, T. A. Springer, and D. E. Staunton. 1994. Residues within a conserved amino acid motif of domains 1 and 4 of VCAM-1 are required for binding to VLA-4. *J. Cell Biol.* 125: 215–222.
28. Clements, J. M., P. Newham, M. Shepherd, R. Gilbert, T. J. Dudgeon, L. A. Needham, R. M. Edwards, L. Berry, A. Brass, and M. J. Humphries. 1994. Identification of a key integrin-binding sequence in VCAM-1 homologous to the LDV active site in fibronectin. *J. Cell Sci.* 107(Pt. 8): 2127–2135.
29. Renz, M. E., H. H. Chiu, S. Jones, J. Fox, K. J. Kim, L. G. Presta, and S. Fong. 1994. Structural requirements for adhesion of soluble recombinant murine vascular cell adhesion molecule-1 to $\alpha_4\beta_1$. *J. Cell Biol.* 125: 1395–1406.
30. Newham, P., S. E. Craig, G. N. Seddon, N. R. Schofield, A. Rees, R. M. Edwards, E. Y. Jones, and M. J. Humphries. 1997. α_4 integrin binding interfaces on VCAM-1 and MAdCAM-1: integrin binding footprints identify accessory binding sites that play a role in integrin specificity. *J. Biol. Chem.* 272: 19429–19440.
31. Rose, D. M., P. M. Cardarelli, R. R. Cobb, and M. H. Ginsberg. 2000. Soluble VCAM-1 binding to α_4 integrins is cell-type specific, activation-dependent, and disrupted during apoptosis in T cells. *Blood* 85: 602–609.

32. Rose, D. M., S. Liu, D. G. Woodside, J. Han, D. D. Schlaepfer, and M. H. Ginsberg. 2003. Paxillin binding to the α_4 integrin subunit stimulates LFA-1 (integrin $\alpha_L\beta_2$)-dependent T cell migration by augmenting the activation of focal adhesion kinase/proline-rich tyrosine kinase-2. *J. Immunol.* 170: 5912–5918.
33. Woodside, D. G., T. K. Teague, and B. W. McIntyre. 1996. Specific inhibition of T lymphocyte coactivation by triggering integrin β_1 reveals convergence of β_1, β_2, and β_7 signaling pathways. *J. Immunol.* 157: 700–706.
34. Vanderslice, P., K. Ren, J. K. Revelle, D. C. Kim, D. Scott, R. J. Bjercke, E. T. Yeh, P. J. Beck, and T. P. Kogan. 1997. A cyclic hexapeptide is a potent antagonist of α_4 integrins. *J. Immunol.* 158: 1710–1718.
35. Szabo, M. C., T. K. Teague, and B. W. McIntyre. 1995. Regulation of lymphocyte pseudopodia formation by triggering the integrin $\alpha_4\beta_1$. *J. Immunol.* 154: 2112–2124.
36. Tsujisaki, M., K. Imai, H. Hirata, Y. Hanzawa, J. Masuya, T. Nakano, T. Sugiyama, M. Matsui, Y. Hinoda, and A. Yachi. 1991. Detection of circulating intercellular adhesion molecule-1 antigen in malignant diseases. *Clin. Exp. Immunol.* 85: 3–8.
37. Reilly, P. L., J. R. Woska, D. D. Jeanfavre, E. McNally, R. Rothlein, and B. J. Bormann. 1995. The native structure of intercellular adhesion molecule-1 (ICAM-1) is a dimer. *J. Immunol.* 155: 529–532.
38. Dando, J., K. W. Wilkinson, S. Ortlepp, D. J. King, and R. L. Brady. 2002. A reassessment of the MAdCAM-1 structure and its role in integrin recognition. *Acta Crystallogr. D Biol. Crystallogr.* 58: 233–241.
39. Chigaev, A., G. Zwartz, S. W. Graves, D. C. Dwyer, H. Tsuji, T. D. Foutz, B. S. Edwards, E. R. Prossnitz, R. S. Larson, and L. A. Sklar. 2003. $\alpha_4\beta_1$ integrin affinity changes govern cell adhesion. *J. Biol. Chem.* 278: 38174–38182.
40. Jones, E. Y., K. Harlos, M. J. Borromley, R. C. Robinson, P. C. Driscoll, R. M. Edwards, J. M. Clements, T. J. Dudgeon, and D. I. Stuart. 1995. Crystal structure of an integrin-binding fragment of vascular cell adhesion molecule-1 at 1.8 A resolution. *Nature* 373: 539–544.
41. Wang, J., R. B. Pepinsky, T. Stehle, J. Liu, M. Karpusas, B. Browning, and L. Osborn. 1995. The crystal structure of an N-terminal two-domain fragment of vascular cell adhesion molecule 1 (VCAM-1); a cyclic peptide based on domain 1 C-D loop can inhibit VCAM-1-α_4 integrin interaction. *Proc. Natl. Acad. Sci. USA* 92: 5714–5718.
42. Redick, S. D., D. L. Settles, G. Briscoe, and H. P. Erickson. 2000. Defining fibronectin's cell adhesion synergy site by site-directed mutagenesis. *J. Cell Biol.* 149: 521–527.
43. Altroff, H., R. Schlinkert, C. F. van der Walle, A. Bernini, I. D. Campbell, J. M. Werner, and H. J. Mardon. 2004. Interdomain tilt angle determines integrin-dependent function of the ninth and tenth FIII domains of human fibronectin. *J. Biol. Chem.* 279: 55995–56003.
44. Taylor, P., M. Bilsland, and M. D. Walkinshaw. 2001. A new conformation of the integrin-binding fragment of human VCAM-1 crystallizes in a highly hydrated packing arrangement. *Acta Crystallogr. D Biol. Crystallogr.* 57: 1579–1583.
45. Pepinsky, B., C. Hession, L. L. Chen, P. Moy, L. Burkly, A. Jakubowski, E. P. Chow, C. Benjamin, G. Chi-Rosso, and S. Luhowskyj. 1992. Structure/function studies on vascular cell adhesion molecule-1. *J. Biol. Chem.* 267: 17820–17826.
46. Bednarczyk, J. L., and B. W. McIntyre. 1990. A monoclonal antibody to VLA-4 α-chain (CDw49d) induces homotypic lymphocyte aggregation. *J. Immunol.* 144: 777–784.
47. Campanero, M. R., R. Pulido, M. A. Ursa, M. Rodriguez Moya, M. O. de Landazuri, and F. Sanchez-Madrid. 1990. An alternative leukocyte homotypic adhesion mechanism, LFA-1/ICAM-1-independent, triggered through the human VLA-4 integrin. *J. Cell Biol.* 110: 2157–2165.
48. Teixido, J., C. M. Parker, P. D. Kassner, and M. E. Hemler. 1992. Functional and structural analysis of VLA-4 integrin α_4 subunit cleavage. *J. Biol. Chem.* 267: 1786–1791.
49. You, T. J., D. S. Maxwell, T. P. Kogan, Q. Chen, J. Li, J. Kassir, G. W. Holland, and R. A. Dixon. 2002. A 3D structure model of integrin $\alpha_4\beta_1$ complex. I. Construction of a homology model of β_1 and ligand binding analysis. *Biophys. J.* 82: 447–457.
50. Qian, F., D. L. Vaux, and I. L. Weissman. 1994. Expression of the integrin $\alpha_4\beta_1$ on melanoma cells can inhibit the invasive stage of metastasis formation. *Cell* 77: 335–347.
51. Swerlick, R. A., J. R. Eckman, A. Kumar, M. Jeitler, and T. M. Wick. 1993. $\alpha_4\beta_1$ integrin expression on sickle reticulocytes: vascular cell adhesion molecule-1-dependent binding to endothelium. *Blood* 82: 1891–1899.
52. Joneckis, C. C., R. L. Ackley, E. P. Orringer, E. A. Wayner, and L. V. Parise. 1993. Integrin $\alpha_4\beta_1$ and glycoprotein IV (CD36) are expressed on circulating reticulocytes in sickle cell anemia. *Blood* 82: 3548–3555.
53. Lutty, G. A., M. Taomoto, J. Cao, D. S. McLeod, P. Vanderslice, B. W. McIntyre, M. E. Fabry, and R. L. Nagel. 2001. Inhibition of TNF-α-induced sickle RBC retention in retina by a VLA-4 antagonist. *Invest. Ophthalmol. Visual Sci.* 42: 1349–1355.
54. Lutty, G. A., T. Otsuji, M. Taomoto, C. Merges, D. S. McLeod, S. Y. Kim, P. Vanderslice, S. Suzuka, M. E. Fabry, and R. L. Nagel. 2002. Mechanisms for sickle red blood cell retention in choroid. *Curr. Eye Res.* 25: 163–171.
55. Setty, B. N., and M. J. Stuart. 1996. Vascular cell adhesion molecule-1 is involved in mediating hypoxia-induced sickle red blood cell adherence to endothelium: potential role in sickle cell disease. *Blood* 88: 2311–2320.